

Article

# Developing Equivalent Consumption Minimization Strategy for Advanced Hybrid System-II Electric Vehicles

Hsiu-Ying Hwang 

Department of Vehicle Engineering, National Taipei University of Technology, Taipei 10608, Taiwan; hhwang@mail.ntut.edu.tw

Received: 24 March 2020; Accepted: 17 April 2020; Published: 19 April 2020



**Abstract:** Compared with conventional vehicles, hybrid electric vehicles (HEVs) have the advantage of high-energy conversion efficiency, which can have better fuel economy and lower emissions. The main issue of HEVs is how to develop an energy management strategy to achieve significantly better fuel efficiency. In this research, the Equivalent Consumption Minimization Strategy (ECMS) was applied to optimize the performance of fuel consumption in the Advanced Hybrid System-II (AHS-II). Based on FTP-75 Test Procedure defined by the U.S. Environmental Protection Agency (EPA), a backward simulation module was established. The baseline simulation module with the rule-based control strategy was validated with the original fuel consumption data. Then, the module with ECMS followed the same control rules of engine on/off and mode selection, and the fuel consumption of ECMS was compared with the simulation results of the baseline model. The fuel economy improvements of ECMS in urban, highway driving pattern, and composite fuel economy were up to 8.5%, 7.7%, and 8.1%, respectively. The simulation results showed that the difference of motors' working efficiency was only 1.2% between ECMS and baseline rule-based control strategies. The main reason of fuel consumption improvement was the engine operation chosen by ECMS, which provided better power distribution.

**Keywords:** hybrid electric vehicles; equivalent consumption minimization strategy; power-split hybrid

## 1. Introduction

Climate change and the sustainable development of energy are the most serious international issues in the 21st century. The hybrid electric vehicle (HEV) is one of the key technologies for vehicle energy saving. Combining with the internal combustion engine (ICE) and high efficiency electric motor, hybrid electric vehicles have better fuel economy than traditional vehicles. The HEVs are also more achievable than electric vehicles (EVs) under current limitations of battery.

With ICE and electric motors, the operating modes to control engine and motors are necessary designs for the hybrid power system, and the switching between the modes would change its power flow and the operation of the components. A planetary gear set (PGS) is often applied to the configuration of HEV. The most representative design is Toyota Prius released in 1997. In 2005, the Advanced Hybrid System-II (AHS-II), also known as the two-mode hybrid system, was developed by General Motors. AHS-II offers an additional set of electric-continue-variable-transmission (eCVT) mode of operation, and significantly reduce the energy loss in high speed [1]. Arata et al. [2] analyzed two different power-split hybrid-electric vehicle (HEV) powertrains using backward-looking simulations, and compared the Toyota Hybrid System II (THS-II) and the General Motors Allison Hybrid System II (GM AHSII).

Fuel economy and lower pollution emissions are critical issues. Vehicle manufactures are investing in energy management strategy (EMS) to ensure that the system components operate in their safe

working range, and, at the same time, to maintain a high energy conversion efficiency to obtain better fuel economy and lower pollution emissions. The EMS can be divided into two categories, rule-based control strategy (RB) and optimization control strategy. Each of these two categories can be further divided into two subcategories. RB is subdivided into fuzzy control and heuristic control, while the optimization strategy is subdivided into global optimization and real-time or online optimization control [3,4]. RB does not require lengthy numerical calculation time [5,6], and can simultaneously monitor a number of parameters, which are usually associated with engine on/off control, and engine and motor operating points [7,8]. However, the fuel consumption is not optimized. For optimization control strategy, the most representative strategy for global optimization is dynamic programming (DP). However, the algorithm requires the information of full driving time, it is difficult to apply for a real vehicle control [9,10]. Chen et al. [11] utilized online control rules but based on offline optimization results of DP for a plug-in HEV to prolong driving range up to 2.86% and reduce the energy consumption up to 5.77%. For real-time optimized control strategy, Equivalent Consumption Minimization Strategy (ECMS) [12] aims at optimal power distribution (between engines and motors) and ensures that the battery pack has sufficient power. Compared to RB, ECMS can have a better fuel economy [13]. Zeng et al. [14] proposed an adaptive simplified-ECMS-based strategy along with particle swarm optimization (PSO) algorithm to optimize PHEV system. The method effectively shortened the calculation time and improved fuel consumption by 16.43%, compared to the Charge Sustaining-Charge Depleting (CS-CD)-based strategy. Dong [15] developed a real-time optimal energy management approach for HEVs and PHEVs using an adaptive coefficient tuning strategy, and validated results using both Model-in-Loop (MIL) and HIL environment. Lu et al. [16] introduced the weighted sum method and no-preference method to solve the multiobjective optimization problem of plug-in electric vehicles and validated with ADVISOR software. Xu et al. [17] developed a fuzzy control strategy for parallel hybrid electric vehicle. The control strategy was adjusted with GA. It was verified that GA could effectively improve the efficiency of the engine and fuel consumption.

This study implemented the AHS-II two-mode system as the transmission structure to establish a Simulink vehicle model, and applied ECMS for EMS to achieve optimal fuel economy.

## 2. Models of Hybrid Electric Vehicle

Two simulation models with the AHS-II two-mode hybrid system were established. One is the baseline model with the rule-based control which would be validated with manufacture official data to verify the accuracy of vehicle model. The other is the optimized vehicle model with ECMS to achieve a better EMS control and optimize fuel efficiency.

### 2.1. Introduction of Hybrid Powertrain System

The AHS-II two-mode hybrid powertrain consists of a planetary gear, a compound planetary gear, four clutches, an internal combustion engine, and two motor/generators, MG1 and MG2, as shown in Figure 1. The architecture can produce effects which are similar to the continuously variable transmission (CVT). Therefore, it is also known as electrical continuously variable transmission (eCVT). The symbols R, S, and C represent the ring gear, the sun gear, and the carrier, respectively, and the subscripts 1 and 2 represent the compound planetary gear set and the simple planetary gear set. When the vehicle travels on different road conditions, the powertrain system can operate between two eCVT modes and four fixed-gear modes.

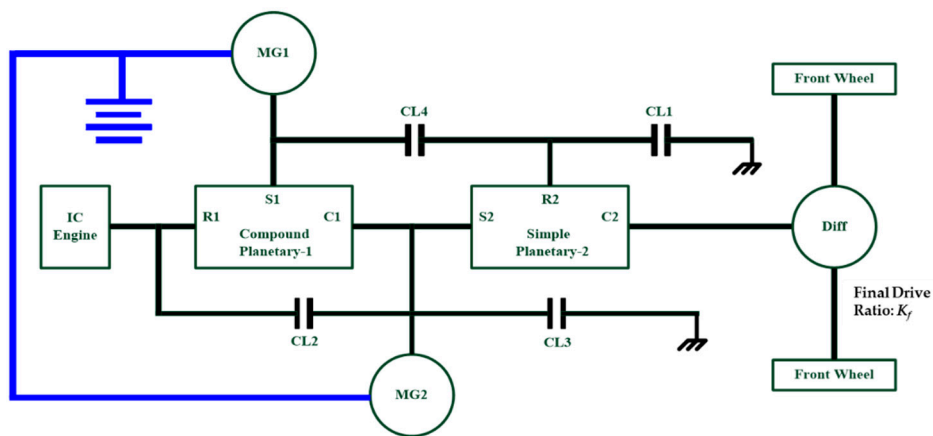


Figure 1. AHS-II two-mode powertrain architecture.

2.2. HEV Simulation Model

The backward calculation dynamic model of the HEV system was implemented using Matlab/Simulink, as shown in Figure 2. The US FTP-75 (EPA Federal Test Procedure) urban and highway drive cycles were applied as the road conditions for simulation, as shown in Figures 3 and 4. According to the known driving speed, the vehicle dynamic model calculated the required vehicle acceleration and driving torque, and through the energy management control module, the operating mode of the system and the output powers of engine and motor/generators, MG1 and MG2, were determined. The speed and torque of the two motor/generators were determined by the gear ratio of the transmission module. According to the speed and torque of the motor/generators, the battery module calculated the state of charge (SOC) of the battery pack. Finally, the fuel consumption was accumulated by ICE module through an engine two-dimensional lookup table.

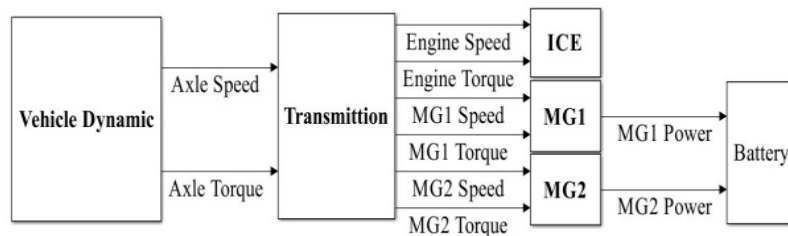


Figure 2. Two-mode powertrain simulation model.

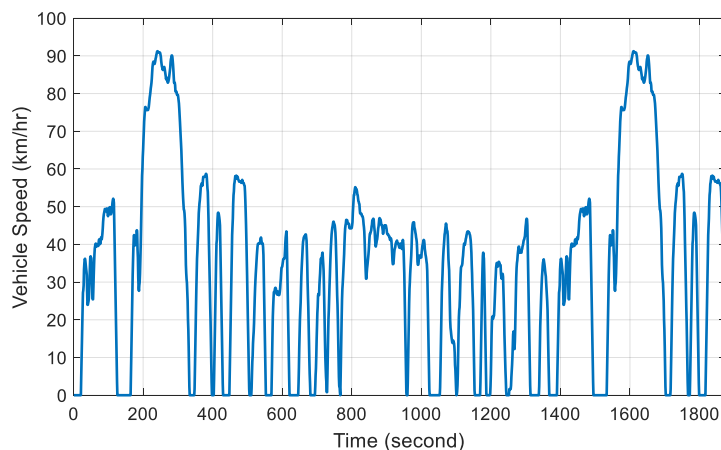


Figure 3. FTP-75 urban driving cycle.

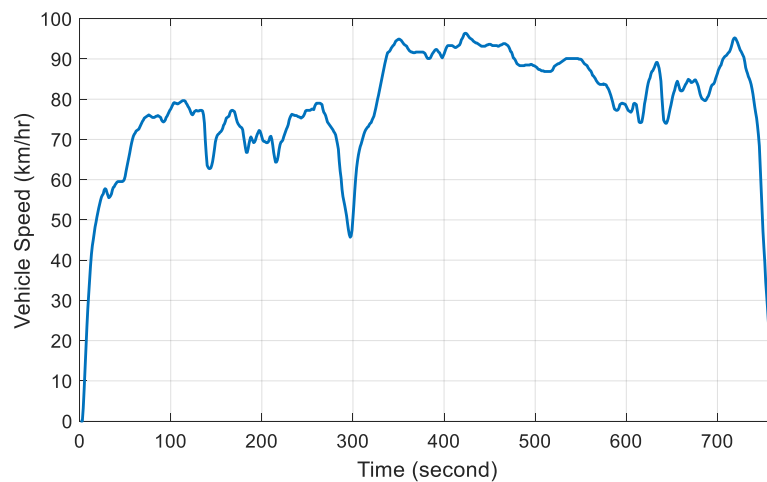


Figure 4. FTP-75 highway driving cycle.

### 2.3. Vehicle Dynamic Module

According to the driving cycle, the vehicle speed was received, and the road load of vehicle model, including rolling resistance, aerodynamic drag, grade resistance, was calculated by Equations (1)–(4). Further, the AHS-II output shaft required torque was obtained. The vehicle parameters are shown in Table 1.

$$F_{Load} = F_r + F_w + F_g, \quad (1)$$

$$F_r = f_r M g \cos \alpha, \quad (2)$$

$$F_w = \frac{1}{2} \rho A_f C_D V^2, \quad (3)$$

$$F_g = M g \sin \alpha, \quad (4)$$

where  $F_{Load}$ ,  $F_r$ ,  $F_w$ , and  $F_g$  are vehicle road load, rolling resistance, aerodynamic drag, and grade resistance, respectively, and  $f_r$ ,  $M$ ,  $g$ ,  $\alpha$ ,  $\rho$ ,  $A_f$ ,  $C_D$ , and  $V$  are rolling resistance coefficient, vehicle mass, gravity, road slope, air density, vehicle front area, aerodynamic drag coefficient, and vehicle speed, respectively.

Table 1. Vehicle parameters for dynamic simulation.

| Item (Unit)                              | Value |
|--|-------|
| Mass (kg)                                | 1600  |
| Radius of the tire (m)                   | 0.352 |
| Vehicle frontal area (m <sup>2</sup> )   | 2.642 |
| Rolling resistance coefficient           | 0.01  |
| Gravity acceleration (m/s <sup>2</sup> ) | 9.81  |
| Aerodynamic drag coefficient             | 0.386 |
| Air density (kg/m <sup>3</sup> )         | 1.29  |

### 2.4. Controller Module

In this study, two sets of controllers were established, the rule-based control module for baseline HEV model and the Equivalent Consumption Minimization Strategy (ECMS) module for the optimized HEV model. These control modules were combined with the engine switch strategy to further determine the operating time of the ICE. The individual controllers were built with Matlab functions.

Based on the torque required for the vehicle driving and the battery SOC, the rule-based controller, heuristic method (if-then-else), determined the speed and torque of ICE. The ESCM with object function

developed the working state of the engine. After determining the status of ICE, the mode switch control module would switch between different eCVT and fixed-gear modes.

### 2.5. Transmission Module

The transmission includes two planetary gear sets, two motor/generators, and four clutches. Based on the vehicle driving condition, the mode switch module would determine the mode of operation, mode 1 for first eCVT mode and mode 2 for second eCVT mode. For mode 1, the motor speeds and torques of MG1 and MG2 were simulated by Equations (5)–(8). Equations (9)–(12) were for mode 2 operation.

$$\omega_{MG1} = \frac{1}{i_1}\omega_e - \frac{(1 - i_1)(1 + i_2)}{i_1 i_2}\omega_{out}, \tag{5}$$

$$\omega_{MG2} = \frac{1 + i_2}{i_2}\omega_{out}, \tag{6}$$

$$T_{MG1} = -i_1 T_e, \tag{7}$$

$$T_{MG2} = -(1 - i_1)T_e + \frac{i_2}{1 + i_2}T_{out}, \tag{8}$$

$$\omega_{MG1} = -\frac{i_2}{1 - i_1 - i_1 i_2}\omega_e + \frac{(1 - i_1)(1 + i_2)}{1 - i_1 - i_1 i_2}\omega_{out}, \tag{9}$$

$$\omega_{MG2} = \frac{1}{1 - i_1 - i_1 i_2}\omega_e - \frac{i_1(1 + i_2)}{1 - i_1 - i_1 i_2}\omega_{out}, \tag{10}$$

$$T_{MG1} = -i_1 T_e + \frac{1}{1 + i_2}T_{out}, \tag{11}$$

$$T_{MG2} = -(1 - i_1)T_e + \frac{i_2}{1 + i_2}T_{out}, \tag{12}$$

where,

$$i_1 = \frac{R_{S1}}{R_{R1}}, \tag{13}$$

$$i_2 = \frac{R_{S2}}{R_{R2}}, \tag{14}$$

$\omega_e$ ,  $\omega_{MG1}$ ,  $\omega_{MG2}$ ,  $\omega_{out}$ ,  $T_e$ ,  $T_{MG1}$ ,  $T_{MG2}$ , and  $T_{out}$  are the rotational speeds and torques of the engine, two motors, and transmission output.  $R_{R1}$ ,  $R_{R2}$ ,  $R_{S1}$  and  $R_{S2}$  are the radii of ring gear 1 and 2 and of sun gear 1 and 2, respectively.  $i_1$ ,  $i_2$  are the radius ratio of sun gear to ring gear for gear train 1 and 2, respectively.

In the simulation, the rotational inertia of engine,  $I_e$ ; inertia of ring gear 1 and 2,  $I_{R1}$  and  $I_{R2}$ ; inertia of carrier 1 and 2,  $I_{C1}$ , and  $I_{C2}$ ; inertia of motor/generator 1 and 2,  $I_{MG1}$  and  $I_{MG2}$ ; and inertia of sun gear 1 and 2,  $I_{S1}$  and  $I_{S2}$ ; are all considered. In mode 1 case, the general force-acceleration matrix can be written as shown in Equation (15). Similarly, Equation (16) is the case of mode 2.

$$\begin{bmatrix} \dot{\omega}_e \\ \dot{\omega}_{out} \\ \dot{\omega}_{MG1} \\ \dot{\omega}_{MG2} \\ F_1 \\ F_2 \end{bmatrix} = \begin{bmatrix} I_e + I_{R1} & 0 & 0 & 0 & R_{R1} & 0 \\ 0 & I_{C2} + \frac{r_{ire}^2}{K_f^2}m & 0 & 0 & 0 & -R_{R2} - R_{S2} \\ 0 & 0 & I_{MG1} + I_{S1} & 0 & -R_{S1} & 0 \\ 0 & 0 & 0 & I_{MG2} + I_{C1} + I_{S2} & -R_{R1} + R_{S1} & R_{S2} \\ R_{R1} & 0 & -R_{S1} & -R_{R1} + R_{S1} & 0 & 0 \\ 0 & -R_{R2} - R_{S2} & 0 & R_{S2} & 0 & 0 \end{bmatrix}^{-1} \begin{bmatrix} T_e \\ -\frac{\Sigma F_{fire}}{K_f}r_{ire} \\ T_{MG1} \\ T_{MG2} \\ 0 \\ 0 \end{bmatrix} \tag{15}$$

$$\begin{bmatrix} \dot{\omega}_e \\ \dot{\omega}_{out} \\ \dot{\omega}_{MG1} \\ \dot{\omega}_{MG2} \\ F_1 \\ F_2 \end{bmatrix} = \begin{bmatrix} I_e + I_{R1} & 0 & 0 & 0 & R_{R1} & 0 \\ 0 & I_{C2} + \frac{r_{tire}^2}{K_f^2} m & 0 & 0 & 0 & -R_{R2} - R_{S2} \\ 0 & 0 & I_{MG1} + I_{S1} + I_{R2} & 0 & -R_{S1} & R_{R2} \\ 0 & 0 & 0 & I_{MG2} + I_{C1} + I_{S2} & -R_{R1} + R_{S1} & R_{S2} \\ R_{R1} & 0 & -R_{S1} & -R_{R1} + R_{S1} & 0 & 0 \\ 0 & -R_{R2} - R_{S2} & R_{R2} & R_{S2} & 0 & 0 \end{bmatrix}^{-1} \begin{bmatrix} T_e \\ -\frac{\Sigma F_{tire}}{K_f} r_{tire} \\ T_{MG1} \\ T_{MG2} \\ 0 \\ 0 \end{bmatrix} \quad (16)$$

where

$$m = M + \frac{I_{wheel}}{r_{tire}^2}. \quad (17)$$

$F_1, F_2,$  and  $F_{tire}$  are the forces acting on the sun gear, ring gear, and tire, respectively.  $K_f$  is the final axle ratio, and  $r_{tire}$  is the radius of tire.  $I_{wheel}$  is the total rotational inertia of the wheels [18].

### 2.6. Internal Combustion Engine Module

The ICE module of this study was represented by a lookup table. Figure 5 shows the three-dimensional ICE fuel consumption rate. Through the controller module to determine the engine running state, the corresponding engine speed and torque could determine engine fuel consumption rate.

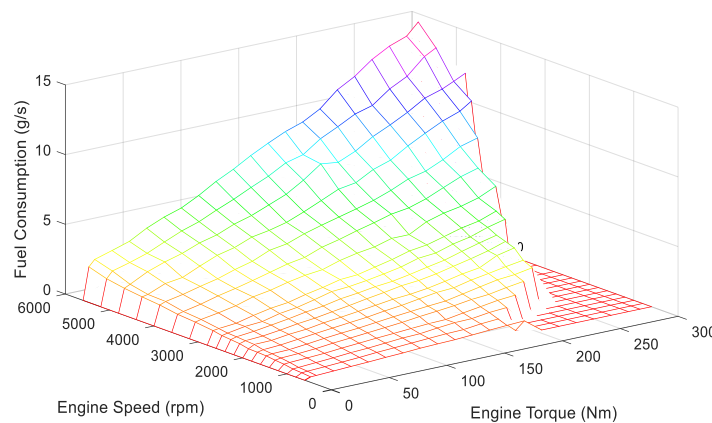


Figure 5. ICE fuel consumption rate.

### 2.7. Motor/Generator Module

In AHS-II powertrain, there are two electric motor/generators, MG1 and MG2, which have same output power. The motor/generators are 60kW permanent magnet AC motors. In this study, MG1 and MG2 had same specifications. The motor/generators efficiency is a function of speed and output torque, as shown in Figure 6. This module was modeled with a lookup table. The motor/generator power calculation is shown in Equation (18).

$$P_{MG} = \omega_{MG} T_{MG} \eta_{MG}^K \begin{cases} K = 1 \\ K = -1 \end{cases} \quad (18)$$

where  $P_{MG}, \omega_{MG},$  and  $T_{MG}$  are motor/generators power, speed, and torque, respectively. If the speed and torque are in the same sign, the motor/generator works as a motor. If the speed and torque are in different sign, the motor/generator works as a generator, which transforms the mechanical energy into electricity and stores in the battery pack.  $\eta_{MG}$  is the efficiency of the motor/generator, and  $K$  is the power flow of the motor/generator.  $K = 1$  is motoring, and  $K = -1$  is generating.

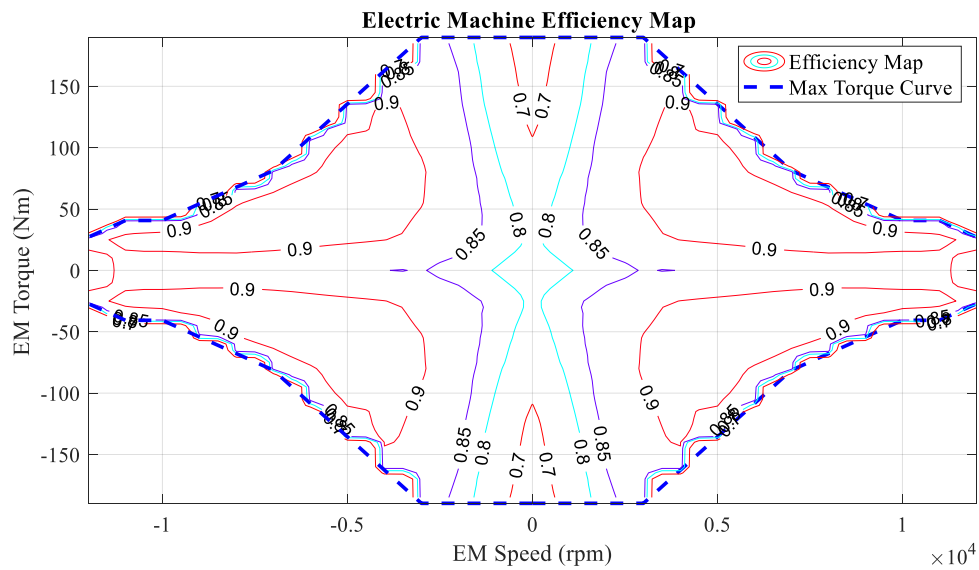


Figure 6. The efficiency of motor/generator.

### 2.8. Battery Module

This study used a battery equivalent circuit, as shown in Figure 7, to establish the battery module [13]. The model provides the information of the open circuit voltage, output voltage, battery current, required power of battery, battery SOC, SOC changing rate, battery internal resistance, and battery capacity. The battery was mainly to support the power required for the motor/generator in order to keep the system in high fuel efficiency. The proposed model was adequate for the fuel consumption optimization.

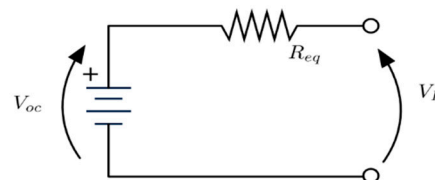


Figure 7. Battery equivalent circuit.

In Figure 7,  $V_{oc}$  is the open circuit voltage,  $R_{eq}$  is the internal equivalent resistance, and  $V_L$  is the output voltage. The power output of battery can be represented in terms of the electric current,  $I_{batt}$ , as shown in Equation (19). The total output of battery,  $V_{oc}I_{batt}$ , includes the power required for the system,  $P_{em\_batt}$ , and the power consumed by the internal resistance of the battery,  $R_{eq}I_{batt}^2$ . The power required can also be represented in terms of motors' power, as shown in Equation (20).

$$P_{em\_batt} = V_{oc}I_{batt} - R_{eq}I_{batt}^2 \tag{19}$$

$$P_{em\_batt} = T_{MG1}\omega_{MG1}\eta_{MG1}^K\eta_{con}^K + T_{MG2}\omega_{MG2}\eta_{MG2}^K\eta_{con}^K, \tag{20}$$

where  $\eta_{MG1}$  and  $\eta_{MG2}$  are the efficiency of the motor/generator 1 and 2,  $\eta_{con}$  is the motor controller efficiency. The battery SOC can be calculated by accumulating the charged and discharged current. The relationship between battery SOC changing rate, battery capacity  $Q_{max}$  and current  $I_{batt}$  is as follows:

$$\dot{SOC}(t) = -\frac{I_{batt}}{Q_{max}}. \tag{21}$$

From Equation (19), the battery current can be derived as follows:

$$I_{batt} = \frac{V_{oc} + \sqrt{V_{oc}^2 - 4R_{eq}P_{em\_batt}}}{2R_{eq}} \quad (22)$$

The open circuit voltage and internal equivalent resistance are function of SOC. From Equations (21) and (22), the SOC rate can be obtained as follows:

$$\dot{SOC}(t) = -\frac{V_{oc}(SOC) + \sqrt{V_{oc}^2(SOC) - 4R_{batt}(SOC)P_{em\_batt}(t)}}{2R_{batt}(SOC)Q_{max}} \quad (23)$$

The internal resistance of battery was based on the curve shown in Figure 8. A portion of the battery power output was provided for the driving system, and the other was consumed by the internal resistance. The efficiency of battery can be calculated, as shown in Equation (24).

$$\eta_{batt} = P_{m\_batt} / V_{oc}I_{batt} \quad (24)$$

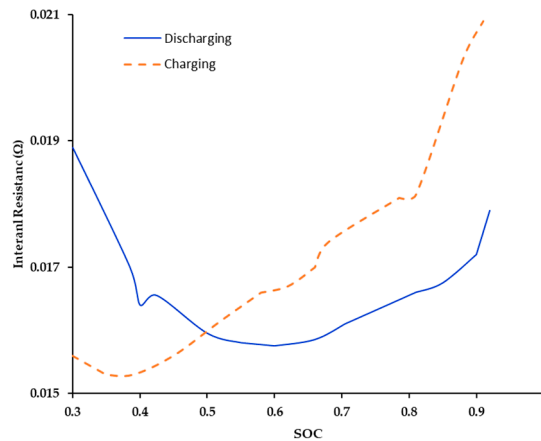


Figure 8. Internal resistance of battery while charging/discharging.

In this study, the SOC of battery was limited in the range between 0.4 and 0.6 since the battery had relatively less energy loss due to the battery internal resistance while considering for both charging and discharging states.

### 3. Energy Management Strategy

#### 3.1. Optimization

The objective of the optimization problem was to minimize the fuel consumption and satisfy the following requirements for the HEV system: (1) To meet the demand of vehicle driving condition, and (2) to be constrained within the operation limits of the system components, as shown in Equations (25)–(30). The goal of the optimization, the cost function  $J$ , is expressed numerically in finite time, as shown in Equation (25). For the hybrid powertrain system with charge-sustaining control, the initial battery SOC and the final state should remain the same. In other words, the power loss of the system must be compensated by the engine. The power required for the vehicle is provided through engine and motors, as shown in Equation (26). Equation (27)–(30) define the SOC controlled limits, battery power output limits, engine power output limits, and motor power output limits, respectively. The optimization problem is defined as the following:

Objective:

$$\min = \left\{ J = \int_{t_0}^{t_f} \dot{m}_{fc}(t) dt \right\}, \quad (25)$$

Subject to

$$P_{req}(t) = P_e(t) + P_{em}(t), \quad (26)$$

$$SOC_{\min} \leq SOC(t) \leq SOC_{\max}, \quad (27)$$

$$P_{em\_batt\_min} \leq P_{em\_batt}(t) \leq P_{em\_batt\_max}, \quad (28)$$

$$P_{e\_min} \leq P_e(t) \leq P_{e\_max}, \quad (29)$$

$$P_{em\_min} \leq P_{em}(t) \leq P_{em\_max}, \quad (30)$$

where  $t$ ,  $J$ ,  $m_{fc}(t)$ ,  $P_{batt}$ ,  $P_e$ ,  $P_{em}$ , and  $P_{req}$  are time, cost function, engine fuel rate, battery power, electric motor power, engine power, and vehicle power required, respectively. In this study, the SOC was limited between 0.4 and 0.6. Battery power and electric motor power were constrained between  $-60$  kW and  $60$  kW. The engine power was between  $0$  kW and  $157$  kW.

### 3.2. Rule-Based Control Strategy

According to the understanding of the system architecture and the efficiency of each element, the output energy of each driving element is defined based on the different road conditions. The basic principle is to meet the driving force required during vehicle travelling, while the control rule should keep the engine and motor/generators in the high operating efficiency range as long as possible to achieve the best fuel consumption and the lowest emissions. This study applied a rule-based controller for the baseline HEV model, and the heuristic was applied, as shown in Figure 9. The fuel economy of this controller would be compared with the manufacture data to verify the accuracy the HEV model. The rule-based strategy is listed in Table 2. Based on different SOC and required torque output, engine operation conditions are provided.

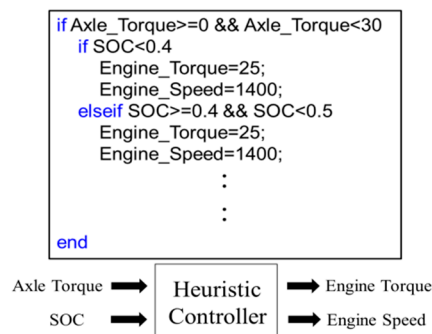


Figure 9. Heuristic controller.

**Table 2.** Rule-based strategy.

| Engine Output<br>Required Torque | SOC < 0.4          | 0.4 ≤ SOC < 0.5    | 0.5 ≤ SOC ≤ 0.6    |
|----------------------------------|--------------------|--------------------|--------------------|
| 0–30 (Nm)                        | 25 Nm<br>1400 rpm  | 25 Nm<br>1400 rpm  | 25 Nm<br>1400 rpm  |
| 30–50 (Nm)                       | 45 Nm<br>1500 rpm  | 45 Nm<br>1500 rpm  | 25 Nm<br>1500 rpm  |
| 50–75 (Nm)                       | 140 Nm<br>1700 rpm | 140 Nm<br>1700 rpm | 100 Nm<br>1700 rpm |
| 75–100 (Nm)                      | 150 Nm<br>1700 rpm | 140 Nm<br>1700 rpm | 130 Nm<br>1700 rpm |
| 100–125 (Nm)                     | 155 Nm<br>1800 rpm | 145 Nm<br>1800 rpm | 130 Nm<br>1800 rpm |
| 125–150 (Nm)                     | 170 Nm<br>1800 rpm | 160 Nm<br>1800 rpm | 160 Nm<br>1800 rpm |
| 150–175 (Nm)                     | 185 Nm<br>1900 rpm | 180 Nm<br>1900 rpm | 170 Nm<br>1900 rpm |
| 175–200 (Nm)                     | 180 Nm<br>2000 rpm | 160 Nm<br>2000 rpm | 140 Nm<br>2000 rpm |
| 200–250 (Nm)                     | 180 Nm<br>2100 rpm | 160 Nm<br>2100 rpm | 140 Nm<br>2100 rpm |
| 250–300 (Nm)                     | 180 Nm<br>2200 rpm | 150 Nm<br>2200 rpm | 130 Nm<br>2200 rpm |
| >300 (Nm)                        |                    | 235 Nm<br>2000 rpm |                    |

### 3.3. Equivalent Consumption Minimization Strategy

ECMS is one of the best optimization control strategies, and ECMS treats the energy storage system, battery pack/supercapacitor as a buffered energy source. The loss of battery power during travel must be recovered from the brake regeneration or the generator driven by the ICE. The cost function of ECMS is shown in Equation (31), which contains the fuel consumption of the ICE and the electricity energy consumption. Since the electricity power consumption and fuel consumption could not be directly compared, electricity power consumption should be converted into the equivalent fuel consumption by Equations (32) and (33).

$$J(t) = \dot{m}_{fc,eqv} = \dot{m}_{fc}(P_c(t)) + \dot{m}_{eqv}(P_{em}(t)), \quad (31)$$

$$\dot{m}_{eqv}(t) = \gamma \cdot s_{dis} \frac{BSFC(t) \cdot P_{em}(t)}{\eta_{batt}(P_{em}) \eta_{em}(P_{em})} + (1 - \gamma) \cdot s_{chg} \cdot \eta_{batt}(P_{em}) \eta_{em}(P_{em}) \cdot BSFC(t) \cdot P_{em}(t), \quad (32)$$

$$\gamma = \frac{1 + \text{sign}(P_{em}(t))}{2}, \quad (33)$$

where  $m_{fc,eqv}$  is the summation of instant fuel consumption,  $m_{eqv}(t)$  is the equivalent fuel consumption of electricity power,  $P_{em}$  is the output power of the motor, and  $s_{dis}$  and  $s_{chg}$  are the equivalent factors of discharging and charging, respectively.  $BSFC$  is the fuel consumption per unit ICE output energy.  $\eta_{batt}$  and  $\eta_{em}$  are the working efficiency of battery pack and motor, respectively.

### 3.4. Engine Switch Control Strategy

In this study, the engine switch was designed to avoid engine operating in high fuel consumption regions and to avoid the overcharging and discharging of the battery pack. Since the battery has less

energy loss due to the internal resistance while the SOC is within 0.4 and 0.6, the design strategy uses this interval as SOC limits. In ECMS, the mode of operation should be determined first. Since the mode 2 is applied to the higher speed, if the SOC does not exceed 0.6, the engine will continue to operate to ensure that the battery system has enough power.

For mode 1 operation, when the vehicle speed is less than 20 km/h, the operating efficiency of engine will be in poor condition. If the SOC is not lower than 0.45, the engine will be shut down and vehicle is driven by electric motor to enhance fuel consumption performance. When the vehicle speed is between 20 km/h and 40 km/h, and the SOC is greater than or equal to 0.55, the engine will be shut down. When the vehicle speed is greater than or equal to 40 km/h, and the SOC is greater than or equal to 0.6, the engine will be shut-down. If SOC is greater than 0.6 and engine remains off, the SOC is monitored and checked until SOC is less than 0.55 and the process is reset to the starting block. The control flowchart of the engine switch is shown in Figure 10. This control logic was applied on the energy management strategies of both HEV models in this study.

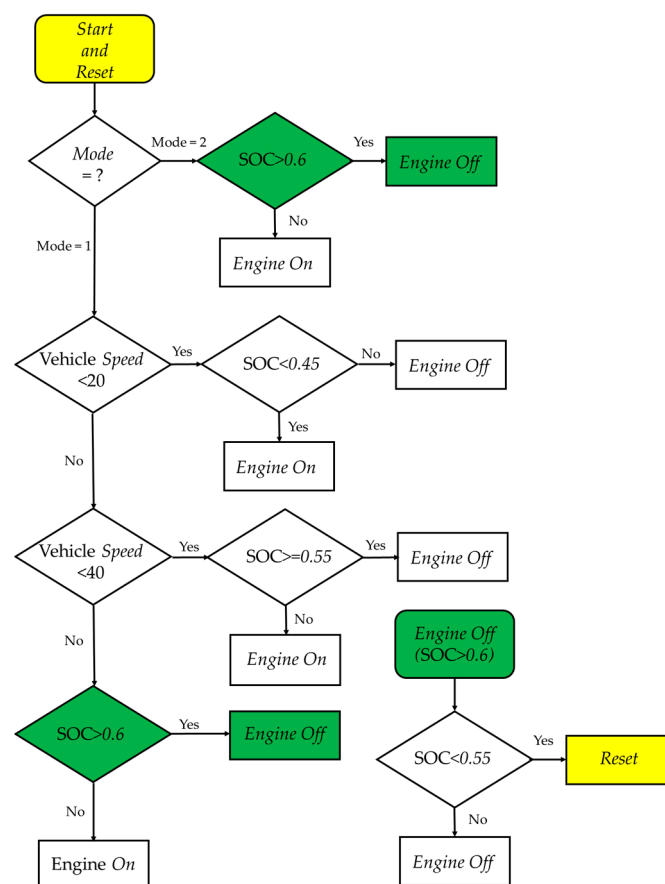


Figure 10. Engine switch flowchart.

## 4. Simulation Results

### 4.1. HEV Baseline Model with Rule-Based Control Strategy

The rule-based control was applied on the baseline HEV model. With the urban and highway driving simulation, fuel economies were 47 MPG (miles per gallon) and 39 MPG, and composite fuel economy was 43 MPG. The simulation results and the manufacture official data are shown in Table 3. The differences of urban, highway, and composite fuel economy were  $-2.1\%$ ,  $5.4\%$ , and  $1.6\%$ , respectively, which were acceptable. The simulation model can be used to represent the original vehicle. With this rule-based control model as the baseline, the average efficiency of MG1 and MG2 were

monitored as well. The urban and highway efficiency values of MG1 were 0.83 and 0.85, respectively, and those of MG2 were 0.85 and 0.84, as shown in Table 4.

**Table 3.** Comparison of fuel consumption between rule-based control model (RB) and factory data.

| Item  | City  | Highway | Composite |
|---|-------|---------|-----------|
| Rule Based (Baseline) (MPG)                         | 47    | 39      | 43        |
| Official Data (MPG)                                 | 48    | 37      | 42        |
| Difference<br>(Rule Based–Official)/Official × 100% | −2.1% | 5.4%    | 1.6%      |

**Table 4.** Motor/generator efficiency in RB.

| Item             | City | Highway |
|------------------|------|---------|
| MG1 (efficiency) | 0.83 | 0.85    |
| MG2 (efficiency) | 0.85 | 0.84    |

#### 4.2. HEV Optimization Model with ECMS

The ECMS was applied as optimization strategy for fuel economy simulation. The result is shown in Table 5. With ECMS, the fuel economy of urban and highways driving cycles had improvements around 8%, while the efficiencies of MG1 and MG2 were tracked as well, as shown in Table 6. The average of urban and highway efficiency values of MG1 were 0.83 and 0.85, and those of MG2 were 0.85 and 0.83, respectively. The difference between the baseline and ECMS was the MG2 highway efficiency, 84% vs. 83%, which was around 1.2% different. Under two different control strategies, the motor/generator efficiencies were very much the same. That indicates the improvement of fuel economy using ECMS was mainly due to the selection of the engine operating points.

**Table 5.** Comparison of fuel consumption between the baseline and equivalent combustion minimization strategy (ECMS).

| Item  | City | Highway | Composite |
|---|------|---------|-----------|
| Baseline (MPG)                                  | 47   | 39      | 43.0      |
| ECMS (MPG)                                      | 51   | 42      | 46.5      |
| Improvement,<br>(ECMS–Baseline)/Baseline × 100% | 8.5% | 7.7%    | 8.1%      |

**Table 6.** Motor/generator efficiency in ECMS.

| Item             | City | Highway |
|------------------|------|---------|
| MG1 (efficiency) | 0.83 | 0.85    |
| MG2 (efficiency) | 0.85 | 0.83    |

Figure 11 to Figure 12 show the engine operating points of baseline and ECMS models. With ECMS optimization, the distribution of the engine operating points in urban and highway driving cycles was significantly smaller than that of the rule-based control strategy. With less engine power during the driving cycles, the ECMS model had less fuel consumption, as shown in Figures 13 and 14.

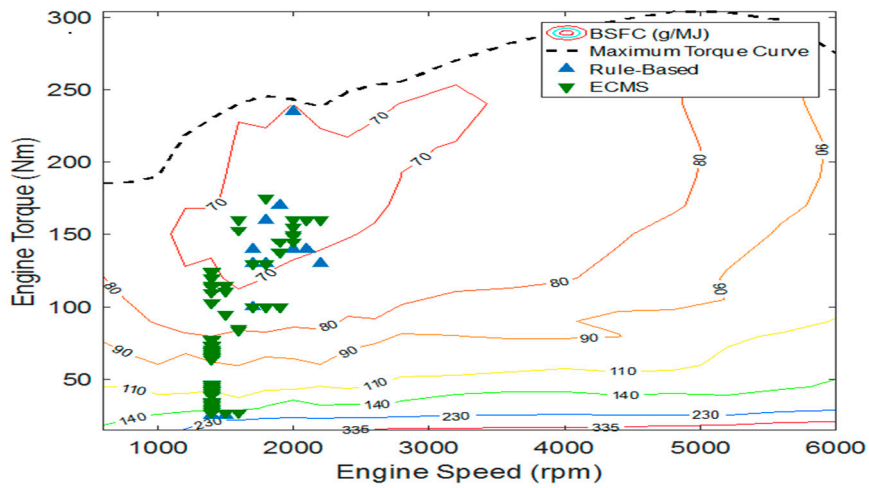


Figure 11. Comparison of engine operating points when driving in urban areas.

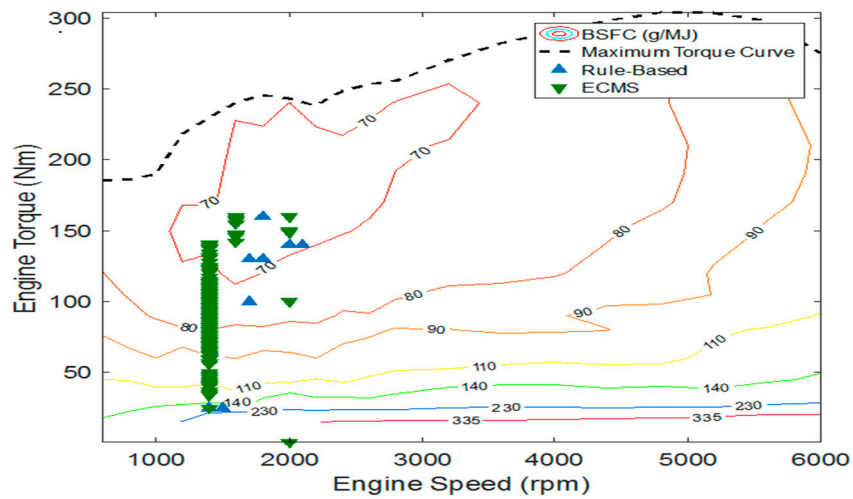


Figure 12. Comparison of engine operating points when driving on expressway.

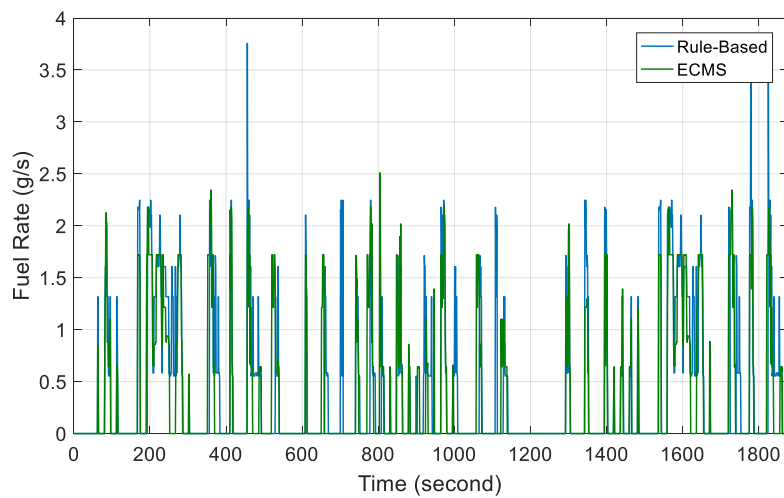


Figure 13. Comparison of fuel consumption rate in urban cycle.

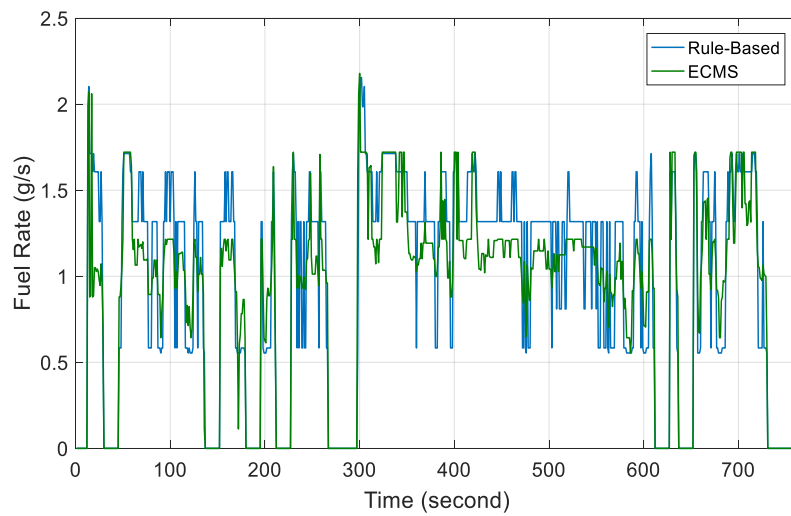


Figure 14. Comparison of fuel consumption rate of highway cycle.

Figures 15 and 16 show the accumulation time of engine operation points in urban driving cycle. The engine load with the rule-based control strategy had up to 42% of the engine running time when operating in the less efficiency range, while the engine load with ECMS had 27% of the engine running time in less efficiency range.

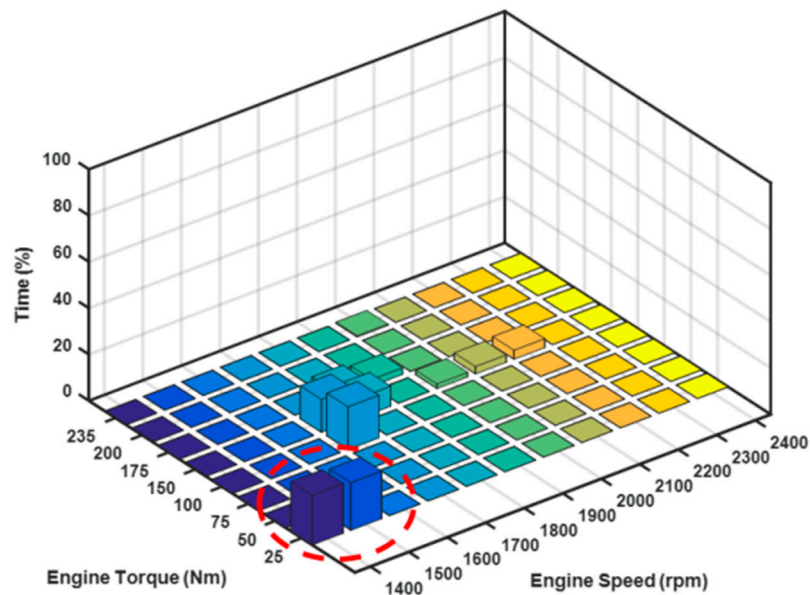
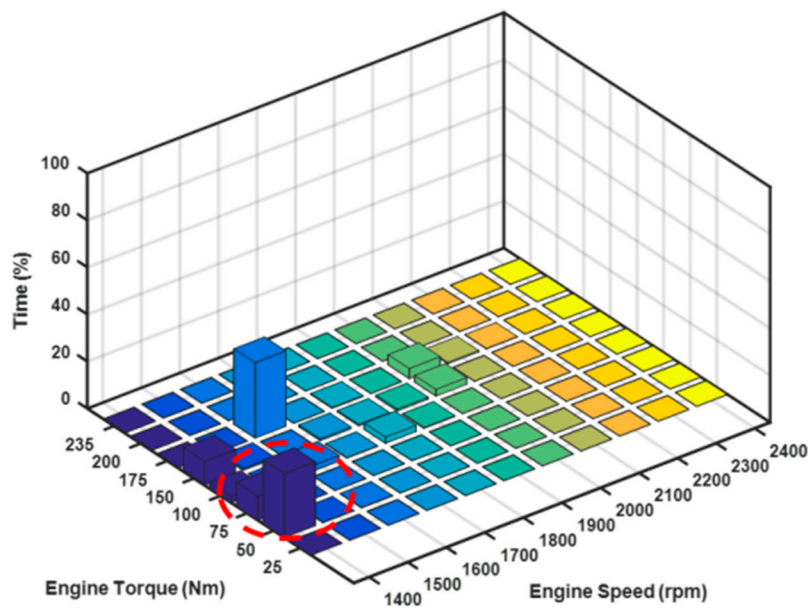
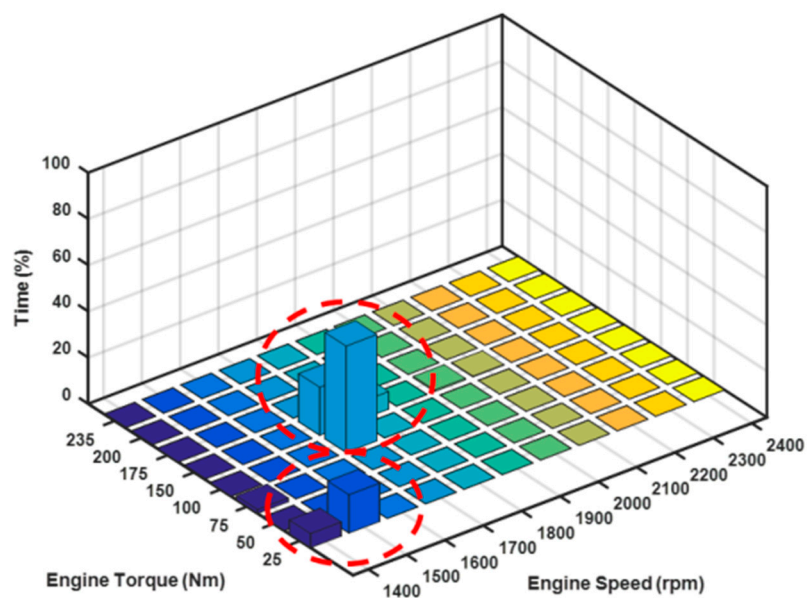


Figure 15. Engine operating time in urban driving cycle with baseline model.



**Figure 16.** Engine operating time in urban driving cycle with ECMS optimization.

In highway driving cycle, as shown in Figures 17 and 18, the engine load with the rule-based control strategy had a significant operating time ratio in the less working efficiency range, accounting for about 22% of the engine operating time, while ECMS did not operate at all in the less efficiency range. With respect to overall operating time, ECMS optimization had a longer running time when operating in the better efficiency range, so HEV model with ECMS optimization could obtain better fuel economy.



**Figure 17.** Engine operating time in highway driving cycle with baseline model.

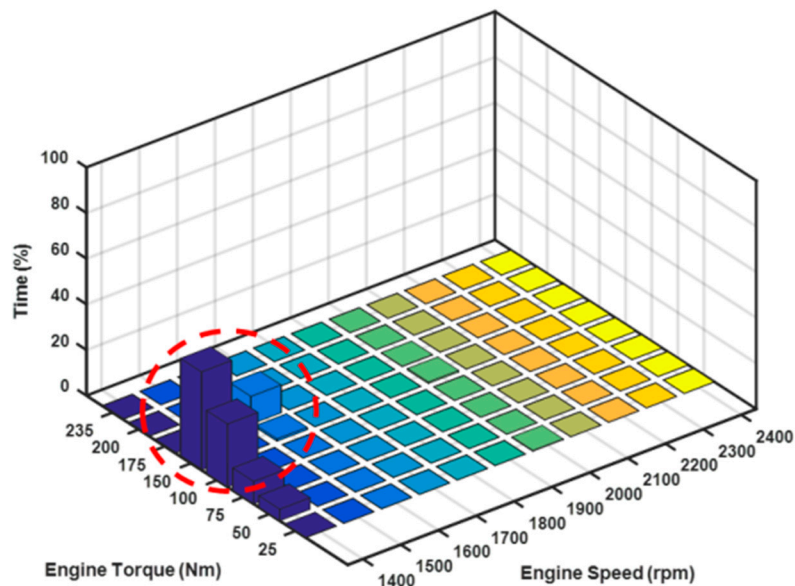


Figure 18. Engine operating time in highway driving cycle with ECMS optimization.

## 5. Conclusions

Energy management strategy is an important topic for hybrid electric vehicles. In order to effectively improve the performance of fuel consumption, ECMS was selected for instant optimization strategy to optimize the fuel consumption.

The AHS-II two-mode hybrid system was modeled, and a rule-based control was used as baseline model and validated with the official fuel economy data. Then, the ECMS was applied for fuel economy optimization. From the simulation of baseline model and ECMS optimization, the conclusions were drawn as follows:

1. For baseline model with the rule-based control strategy, the fuel economy of the urban, highway, and composite driving cycles were 47 MPG, 39 MPG, and 43 MPG. The official reported fuel economy data of AHS-II are 48 MPG, 37 MPG, and 42 MPG for the urban, highway, and composite driving cycle, respectively. The maximum difference of fuel economy between simulation and vehicle official data is 5.4%, which indicates that the results of simulation model has good correlation with those of the vehicle, and can be used to represent the original vehicle.
2. The fuel economies with ECMS optimization were 51 MPG, 42 MPG, and 46.5 MPG for urban, highway, and composite driving cycles, respectively. Comparing ECMS optimization with the rule-based control strategy, the improvements made were 8.5%, 7.7%, and 8.1%, separately. The proposed ECMS optimization strategy provided a better fuel economy performance.
3. The efficiencies of the motor/generator 1 and 2 in the rule-based model were 0.83 and 0.85 for city, and 0.85 and 0.84 for the highway driving cycles. Those in ECMS were 0.83 and 0.85 for city, and 0.85 and 0.83 for highway, individually. The biggest difference between the baseline and ECMS was only 1.2%. The improvement of fuel economy was mainly due to the selection of the engine operating points which lead to a better fuel performance. ECMS could effectively implement the best engine power distribution to achieve better fuel consumption.
4. In urban driving cycle, there was 42% of time that engine was operated in the less efficiency region for the rule-based control strategy, while there was 27% with ECMS.
5. In highway driving cycle, there was 22% of the time that engine was operated in the less efficiency region for the rule-based control strategy, while there were none for ECMS. Overall, ECMS optimization had engine operated in better efficiency range and provided better fuel economy.

Using vehicle dynamic simulation can help to quickly carry out the preliminary evaluation of various energy management strategies, search for the appropriate optimization of energy management strategies, and reduce R&D process time and cost. The proposed equivalent consumption minimization strategy can be utilized to optimize the performance of fuel consumption.

**Funding:** This research received no external funding.

**Conflicts of Interest:** The author declares no conflict of interest.

## Nomenclature

|               |   |
|---------------|---|
| $A_f$         | vehicle front area  |
| AHS-II        | Advanced Hybrid System-II                                       |
| $C_D$         | aerodynamic drag coefficient                                    |
| CVT           | continuously-variable-transmission                              |
| DP            | dynamic programming   |
| ECMS          | Equivalent Consumption Minimization Strategy                    |
| EMS           | energy management strategy                                      |
| EPA           | Environmental Protection Agency                                 |
| eCVT          | electric-continue-variable-transmission                         |
| $F_1$         | force acting on sun gear  |
| $F_2$         | force acting on ring gear                                       |
| $F_g$         | grade resistance  |
| $F_{Load}$    | vehicle road load   |
| $F_r$         | rolling resistance  |
| $F_w$         | aerodynamic drag  |
| $f_r$         | rolling resistance coefficient                                  |
| $F_{tire}$    | force acting on tire  |
| $g$           | gravity   |
| HEVs          | hybrid electric vehicles  |
| $I_{batt}$    | battery current   |
| $I_{C1}$      | rotational inertia of carrier 1                                 |
| $I_{C2}$      | rotational inertia of carrier 2                                 |
| $I_e$         | rotational inertia of engine                                    |
| $I_{MG1}$     | rotational inertia of motor/generator 1                         |
| $I_{MG2}$     | rotational inertia of motor/generator 2                         |
| $I_{R1}$      | rotational inertia of ring gear 1                               |
| $I_{R2}$      | rotational inertia of ring gear 2                               |
| $I_{S1}$      | rotational inertia of sun gear 1                                |
| $I_{S2}$      | rotational inertia of sun gear 2                                |
| $I_{wheel}$   | total rotational inertia of the wheels                          |
| ICE           | internal combustion engine                                      |
| $J$           | cost function   |
| $K$           | power flow of the motor/generator (1: motoring; -1: generating) |
| $K_f$         | final axle ratio  |
| $M$           | vehicle mass  |
| MG            | motor/generators  |
| MPG           | mile per gallon   |
| $m_{eqv}(t)$  | equivalent fuel consumption of electricity power                |
| $m_{fc}(t)$   | engine fuel rate  |
| $m_{fc, eqv}$ | summation of instant fuel consumption                           |
| PHEV          | plug-in hybrid electric vehicle                                 |
| $P_{batt}$    | power output of battery   |
| $P_e$         | output power of the engine                                      |
| $P_{em}$      | output power of the electric motor                              |

|                |  |
|----------------|--|
| $P_{req}$      | vehicle power required                       |
| $P_{MG}$       | motor/generators power                       |
| PGS            | planetary gear set                           |
| $Q_{max}$      | battery capacity                             |
| $R_{eq}$       | internal equivalent resistance               |
| $R_{R1}$       | radius of ring gear 1                        |
| $R_{R2}$       | radius of ring gear 2                        |
| $R_{S1}$       | radius of sun gear 1                         |
| $R_{S2}$       | radius of sun gear 2                         |
| RB             | rule-based control strategy                  |
| $r_{tire}$     | radius of tire                               |
| SOC            | state of charge                              |
| $s_{dis}$      | equivalent factors of discharging            |
| $s_{chg}$      | equivalent factors of charging               |
| $T_e$          | torques of the engine                        |
| $T_{MG}$       | motor/generators torque                      |
| $T_{MG1}$      | torques of the motor 1                       |
| $T_{MG2}$      | torques of the motor 2                       |
| $T_{out}$      | torques of the transmission output           |
| $t$            | time   |
| $V$            | vehicle speed                                |
| $V_{oc}$       | open circuit voltage                         |
| $\alpha$       | road slope                                   |
| $\eta_{batt}$  | working efficiency of battery pack           |
| $\eta_{con}$   | motor controller efficiency                  |
| $\eta_{em}$    | working efficiency of motor                  |
| $\eta_{MG}$    | efficiency of the motor/generator            |
| $\eta_{MG1}$   | efficiency of the motor/generator 1          |
| $\eta_{MG2}$   | efficiency of the motor/generator 2          |
| $\rho$         | air density                                  |
| $\omega_e$     | rotational speeds of the engine              |
| $\omega_{MG}$  | motor/generators speed                       |
| $\omega_{MG1}$ | rotational speeds of the motor 1             |
| $\omega_{MG2}$ | rotational speeds of the motor 2             |
| $\omega_{out}$ | rotational speeds of the transmission output |

## References

1. Meisel, J. An Analytic Foundation for the Two-Mode Hybrid-Electric Powertrain with a Comparison to the Single-Mode Toyota Prius THS-II Powertrain. In Proceedings of the 2009 SAE World Congress, Detroit, MI, USA, 20–23 April 2009. SAE Paper No.2009-01-1321.
2. Arata, J.; Leamy, M.J.; Meisel, J.; Cunefare, K.; Taylor, D. Backward-Looking Simulation of the Toyota Prius and General Motors Two-Mode Power-Split HEV Powertrains. In Proceedings of the 2011 the SAE World Congress, Detroit, MI, USA, 12–14 April 2011. SAE Paper No.2011-01-0948.
3. Salmasi, F.R. Control Strategies for Hybrid Electric Vehicles Evolution Classification, Comparison and Future Trends. *IEEE Trans. Veh. Technol.* **2007**, *56*, 2393–2404. [[CrossRef](#)]
4. Wirasingha, S.G.; Emadi, A. Classification and Review of Control Strategies for Plug-In Hybrid Electric Vehicles. *IEEE Trans. Veh. Technol.* **2011**, *60*, 111–122. [[CrossRef](#)]
5. Mansour, C.J. Trip-Based Optimization Methodology for a Rule-Based Energy Management Strategy Using a Global Optimization Routine: The Case of the Prius Plug-in Hybrid Electric Vehicle. *Proc. Inst. Mech. Eng. Part D J. Automob. Eng.* **2015**, *230*, 1529–1545. [[CrossRef](#)]
6. Peng, J.; He, H.; Xiong, R. Rule Based Energy Management Strategy for a Series-Parallel Plug-In Hybrid Electric Bus Optimized by Dynamic Programming. *J. Appl. Energy* **2017**, *185*, 1633–1643. [[CrossRef](#)]

7. Moulik, B.; Söffker, D. Optimal Rule-Based Power Management for Online, Real-Time Applications in Hevs with Multiple Sources and Objectives: A Review. *J. Energies* **2015**, *8*, 9049–9063. [[CrossRef](#)]
8. Cheng, Y.; Cui, S.; Chan, C.C. Control Strategies for an Electric Variable Transmission Based Hybrid Electric Vehicle. In Proceedings of the 5th IEEE Vehicle Power and Propulsion Conference (VPPC'09), Dearborn, MI, USA, 7–11 September 2009; pp. 1296–1300.
9. Wang, R.; Lukic, S.M. Dynamic Programming Technique in Hybrid Electric Vehicle Optimization. In Proceeding of the 2012 IEEE International Electric Vehicle Conference Electric Vehicle Conference (IEVC), Greenville, SC, USA, 4–8 March 2012; pp. 1–8.
10. Pisu, P.; Rizzoni, G. A comparative study of supervisory control strategies for hybrid electric vehicles. *IEEE Trans. Contr. Syst. Technol.* **2007**, *15*, 506–518. [[CrossRef](#)]
11. Chen, Z.; Liu, W.; Yang, Y.; Chen, W. Online Energy Management of Plug-In Hybrid Electric Vehicles for Prolongation of All-Electric Range Based on Dynamic Programming. *Math. Probl. Eng.* **2015**, *2015*, 368769. [[CrossRef](#)]
12. Yuan, Z.; Teng, L.; Fengchun, S.; Peng, H. Comparative Study of Dynamic Programming and Pontryagin's Minimum Principle on Energy Management for a Parallel Hybrid Electric Vehicle. *J. Energies* **2013**, *6*, 2305–2318. [[CrossRef](#)]
13. Gao, J.P.; Zhu, G.M.; Strangas, E.G.; Sun, F.C. Equivalent Fuel Consumption Optimal Control of a Series Hybrid Electric Vehicle. *Proc. Inst. Mech. Eng. Part D J. Automob. Eng.* **2009**, *223*, 1003–1018. [[CrossRef](#)]
14. Zeng, Y.; Cai, Y.; Kou, G.; Gao, W.; Qin, D. Energy Management for Plug-In Hybrid Electric Vehicle Based on Adaptive Simplified-ECMS. *Sustainability* **2018**, *10*, 2060. [[CrossRef](#)]
15. Dong, J. Modeling and Real-Time Optimal Energy Management for Hybrid and Plug-in Hybrid Electric Vehicles. Ph.D. Thesis, Tongji University, Shanghai, China, 2009.
16. Lu, X.; Chen, Y.; Wang, H. Multi-Objective Optimization Based Real-Time Control for PEV Hybrid Energy Management Systems. In Proceedings of the IEEE Applied Power Electronics Conference and Exposition (APEC), San Antonio, TX, USA, 4–8 March 2018; pp. 969–975.
17. Xu, Q.; Luo, X.; Jiang, X.; Zhao, M. Research on Double Fuzzy Control Strategy for Parallel Hybrid Electric Vehicle Based on GA and DP Optimization. *IET Electr. Syst. Transp.* **2018**, *8*, 144–151. [[CrossRef](#)]
18. Ehsani, M.; Gao, Y.; Emadi, A. *Modern Electric, Hybrid Electric, and Fuel Cell Vehicles: Fundamentals, Theory, and Design*, 2nd ed.; CRC Press Taylor&Francis Group: Boca Raton, FL, USA, 2010.



© 2020 by the author. Licensee MDPI, Basel, Switzerland. This article is an open access article distributed under the terms and conditions of the Creative Commons Attribution (CC BY) license (<http://creativecommons.org/licenses/by/4.0/>).